Decay properties and photodetachment of the diatomic oxygen ion O_2^- in a constant electric field

Jin-Wook Jung, Kyungsun Na, and Linda E. Reichl
Department of Physics and the Center for Complex Quantum Systems, The University of Texas at Austin, Austin, Texas 78712, USA
(Received 26 February 2009; published 29 July 2009)

The dynamics of the O_2^- ion in a constant electric field is modeled in terms of a complex spectral decomposition of the energy Green's function for this open system. The survival probability of the excess electron in the presence of the constant field and the photodetachment rate of the electron in the presence of a radiation field are computed.

DOI: 10.1103/PhysRevA.80.012518 PACS number(s): 31.70.Hq, 32.80.Gc, 02.90.+p

I. INTRODUCTION

The mechanisms leading to the formation of metastable states and decay processes in molecular systems are elusive because of the complexity of the molecular dynamics that give rise to those decay processes. These mechanisms are important because they govern the dynamics of chemical reactions and the dynamics of molecular scattering processes.

The formation of metastable states in atomic systems is more accessible and considerable work has been done, in particular, on understanding the destabilizing effects of constant external fields on atomic systems. The effect of constant external electric fields on the photodetachment of atomic ions is particularly striking and has been studied both experimentally [1–4] and theoretically [5–9]. In the presence of a constant external electric field the photodetachment rate, as a function of frequency of an applied monochromatic radiation field, exhibits oscillatory behavior above the threshold for photodetachment and a nonvanishing value below the threshold for photodetachment. Experiment and theoretical predictions are in good agreement. The oscillations are attributed to the interference between the emitted electron wave traveling toward and reflected from the potential wall caused by the presence of the constant electric field.

Until now, not much attention has been given to the photodetachment rate of molecular ions in the presence of a constant electric field. The effect of vibration on the photodetachment of the excess electron in O_2^- has been studied in the absence of a constant electric field [10].

In this paper we consider a model that can describe the decay and photodetachment of the excess electron in the O_2^- ion in the presence of a constant electric field. We assume that the electric field is directed along the axis of the molecule, and we describe the attractive interaction between the electron and the oxygen atoms in terms of delta-function attractive potential wells (delta potentials). This model of O_2^- is a generalization of work by Ludviksson [11] and by Nickel and Reichl [12]. Ludviksson showed that singularities of the energy Green's function for a particle in a delta potential and constant force field could be found analytically in some parameter ranges. Nickel and Reichl used Ludviksson's model to develop a complex spectral decomposition of the energy Green's function and used the complex spectral decomposition to compute the survival probability of the particle. Emmanouilidou and Reichl later [9] used this spectral decomposition to compute Wigner delay times for an electron scattering from an H atom in the presence of a constant electric field and the photodetachment rate of the excess electron in H^- in the presence of a monochromatic radiation field.

In subsequent sections, we use a generalization of the Ludviksson model to compute the survival probability for the excess electron in the O_2^- ion in the presence of a constant electric field directed along the axis of the molecule. We also compute the photodetachment rate when a radiation field is applied to this system. It is important to note that for this study we neglect the vibrational modes of O_2^- and focus only on the effect of the new metastable states induced by the constant field. Experimental measurements have been made for the photodetachment rate in the absence of a constant field and it is found that vibrations lead to additional peaks as the radiation field frequency becomes commensurate with the vibration frequency [10]. In a subsequent section we will discuss how the constant electric field can contribute to our computed photodetachment rates.

We begin in Sec. II by deriving the model Hamiltonian for O_2^- in a constant electric field. In Sec. III, we derive and analyze the energy Green's function for this molecular system, and in Sec. IV, we show the complex pole structure of the energy Green's function and the behavior of the residues of the poles. In Sec. V, we construct complex eigenstates and compute the survival probability of the excess electron in O_2^- for the system with one bound state. In Sec. VI, we compute the photodetachment rate of the excess electron in the presence of a radiation field. In Sec. VII, we extend the survival probability and photodetachment rate analysis for the system with two bound states. In Sec. VIII, we make concluding remarks.

II. HAMILTONIAN

When a constant electric field is applied parallel to the axis of the O_2^- ion, the dynamics of the excess electron in the ion can be modeled as a one-dimensional system within which the attractive force between the excess electron and each O atom is approximated by an attractive delta potential. The Hamiltonian for the excess electron can be written as

$$\mathcal{H} = -\frac{\hbar^2}{2m}\frac{d^2}{dx^2} - Fx + V_1\delta(x - x_1) + V_2\delta(x - x_2), \qquad (1)$$

where $\hbar$ is Planck's constant, m is the mass of the excess electron, and F is the strength of the constant electric field. The delta potentials are located at $x=x_1$ and $x=x_2$ (the location of the O atoms), and V_j $(j=1,2)$ is the strength of the delta potential at $x=x_j$ and is negative.

We can write the Hamiltonian in terms of dimensionless units. If we define the unit of length to be the Bohr radius $a_0=0.529\ 18$ Å and the unit of energy to be $\epsilon_0 \equiv \frac{\hbar^2}{2ma_0^2}$, then we can define dimensionless variables as follows

$$H \equiv \frac{\mathcal{H}}{\epsilon_0}, \quad \xi \equiv \frac{x}{a_0}, \quad \xi_j \equiv \frac{x_j}{a_0}, \quad d \equiv \frac{|x_2 - x_1|}{a_0},$$

$$\Omega_j \equiv \frac{V_j}{\epsilon_0 a_0}, \quad b \equiv \frac{Fa_0}{\epsilon_0}, \qquad (2)$$

where $j=1,2$. In terms of these dimensionless variables, the dimensionless Hamiltonian takes the form

$$H = -\frac{d^2}{d\xi^2} - b\xi + \Omega_1\delta(\xi - \xi_1) + \Omega_2\delta(\xi - \xi_2). \qquad (3)$$

A schematic diagram of the potential energy in this model is shown in Fig. 1(a) for $\xi_1=0$ and $\xi_2=d$.

There are two parameters we must consider when using our model to describe the O_2^- ion: the internuclear distance d between the two O atoms and the electron affinity of the molecule. If we set $b=0$ and $\Omega_1=\Omega_2=\Omega$ in Eq. (3), then we have a model for O_2^- in the absence of the electric field, if d and Ω are chosen correctly. As shown in Gasiorowicz [13], Eq. (3) with $b=0$ and $\Omega_1=\Omega_2=\Omega$ has two bound states (one symmetric and one antisymmetric) when $2/|\Omega| < d$, and only one bound state (symmetric) when $2/|\Omega| \geq d$. For the symmetric bound state, the delta-function strength and the bound-state energy E_b are related by the equation, $-2\sqrt{|E_b|}/\Omega = 1 + \exp(-\sqrt{|E_b|}d)$ [13]. The spacing between the O atoms is $x_2 - x_1 = 1.207\ 52$ Å [14], which is $d=2.281\ 88$ in dimensionless units. The electron affinity of O_2 is $E_{aff}=0.45$ eV, or in dimensionless units $E'_{aff}=0.033\ 07$. If we equate the electron affinity to the bound-state energy of the symmetric state, then $-2\sqrt{E'_{aff}}/\Omega = 1 + \exp(-\sqrt{E'_{aff}}d)$ and we obtain $\Omega=-0.219\ 067$. In Fig. 1(b), we plot the wave function of the excess electron symmetric bound state $\phi_0(\xi)$ for O_2^- with $b=0$. We will use this state in later sections.

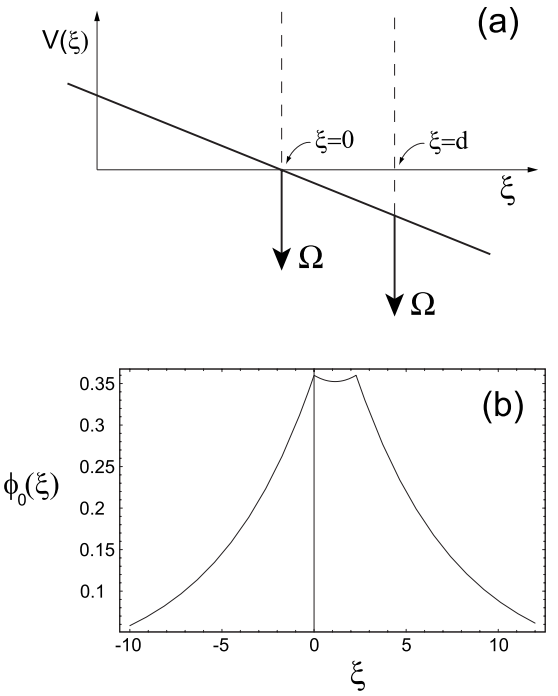

FIG. 1. (a) Schematic diagram for the potential-energy field seen by the excess electron. One delta function is located at $\xi=0$, and the other is located at $\xi=d$. (b) The single bound state of the excess electron for $F=0$. With $\Omega=-0.219\ 067$ and $d=2.281\ 88$, the energy of this bound state is $E'=-0.033\ 074\ 4$, which is the (dimensionless) electron affinity of the excess electron in O_2^-.

We also need to set the value for the constant electric field strength F. We will use the experimental value used in Stewart *et al.* [2], $F/q = 1.43\times10^5$ V/cm, where q is the electron charge, for their experiment on the H^- ion. This gives $b=0.000\ 055\ 618\ 1$ for the dimensionless field strength.

III. ENERGY GREEN'S FUNCTION

We compute the retarded (G^+) and advanced (G^-) energy Green's functions $G^{\pm}(\xi,\xi';E)=\langle\xi|(E-H\pm i\delta)^{-1}|\xi'\rangle$ in a manner similar to that used in [9,11,12] although our result will be more complicated. First, we divide the Hamiltonian into an unperturbed part $H_0=-\frac{d^2}{d\xi^2}-b\xi$ and a perturbation $V(\xi)=+\Omega_1\delta(\xi-\xi_1)+\Omega_2\delta(\xi-\xi_2)$. We will use the notation

$$G(\xi,\xi';z) = \begin{cases} G^+(\xi,\xi';z), & \text{if } \mathrm{Im}(z) > 0, \\ G^-(\xi,\xi';z), & \text{if } \mathrm{Im}(z) < 0. \end{cases} \qquad (4)$$

The energy Green's function for the unperturbed system, $G_0^{\pm}(\xi,\xi';E)=\langle\xi|(E-H_0\pm i\delta)^{-1}|\xi'\rangle$, is given by

$$G_0^{\pm}(\xi,\xi';z) = \begin{cases} -\frac{\pi}{b}\mathrm{Ci}^{\pm}\left(-b\xi' - \frac{z}{b^2}\right)\mathrm{Ai}\left(-b\xi - \frac{z}{b^2}\right), & \text{if } \xi < \xi', \\ -\frac{\pi}{b}\mathrm{Ai}\left(-b\xi' - \frac{z}{b^2}\right)\mathrm{Ci}^{\pm}\left(-b\xi - \frac{z}{b^2}\right), & \text{if } \xi > \xi', \end{cases} \qquad (5)$$

where $\mathrm{Ci}^{\pm}(z) \equiv \mathrm{Bi}(z) \pm i\mathrm{Ai}(z)$, and is basically the same as that used in [9,12] except for a modification in the argument of the Airy functions, Ai and $\mathrm{Ci}^{\pm}$, due to our different definition of the dimensionless parameters.

The Green's function $G(\xi,\xi';z)$ is given by the equation

$$G(\xi,\xi';z) = G_0(\xi,\xi';z) + \int d\xi'' G_0(\xi,\xi'';z)V(\xi'')G(\xi'',\xi';z)$$
$$= G_0(\xi,\xi';z) + \sum_{n=1}^{2} \Omega_n G_0(\xi,\xi_n;z)G(\xi_n,\xi';z). \quad (6)$$

If we set $\xi=\xi_m$ $(m=1,2)$ in Eq. (6) and introduce the following matrices

$$\mathbf{g} \equiv \begin{pmatrix} \mathbf{g}^1 \\ \mathbf{g}^2 \end{pmatrix} \equiv \begin{pmatrix} G(\xi_1,\xi';z) \\ G(\xi_2,\xi';z) \end{pmatrix}, \quad \mathbf{g}_0 \equiv \begin{pmatrix} \mathbf{g}_0^1 \\ \mathbf{g}_0^2 \end{pmatrix} \equiv \begin{pmatrix} G_0(\xi_1,\xi';z) \\ G_0(\xi_2,\xi';z) \end{pmatrix},$$

$$\mathbf{U} \equiv \begin{pmatrix} \mathbf{U}^{11} & \mathbf{U}^{12} \\ \mathbf{U}^{21} & \mathbf{U}^{22} \end{pmatrix} \equiv \begin{pmatrix} \Omega_1 G_0(\xi_1,\xi_1;z) & \Omega_2 G_0(\xi_1,\xi_2;z) \\ \Omega_1 G_0(\xi_2,\xi_1;z) & \Omega_2 G_0(\xi_2,\xi_2;z) \end{pmatrix}, \quad (7)$$

then Eq. (6) can be expressed in matrix form as $\mathbf{g}=\mathbf{g}_0+\mathbf{U}\mathbf{g}$. We solve for $\mathbf{g}$ and obtain

$$\mathbf{g} = (\mathbf{I}-\mathbf{U})^{-1}\mathbf{g}_0$$
$$= \begin{pmatrix} 1-\mathbf{U}^{11} & -\mathbf{U}^{12} \\ -\mathbf{U}^{21} & 1-\mathbf{U}^{22} \end{pmatrix}^{-1} \mathbf{g}_0$$
$$= \frac{1}{(1-\mathbf{U}^{11})(1-\mathbf{U}^{22})-\mathbf{U}^{12}\mathbf{U}^{21}} \begin{pmatrix} 1-\mathbf{U}^{22} & \mathbf{U}^{12} \\ \mathbf{U}^{21} & 1-\mathbf{U}^{11} \end{pmatrix} \begin{pmatrix} \mathbf{g}_0^1 \\ \mathbf{g}_0^2 \end{pmatrix}. \quad (8)$$

After some algebra, we can finally write the retarded (+) and advanced (−) energy Green's functions $G^{\pm}(\xi,\xi';z)$ in the form

$$G^{\pm}(\xi,\xi';z) = G_0^{\pm}(\xi,\xi';z) + \frac{1}{\left(\frac{1}{\Omega_1}-G_0^{\pm}(\xi_1,\xi_1;z)\right)\left(\frac{1}{\Omega_2}-G_0^{\pm}(\xi_2,\xi_2;z)\right)-[G_0^{\pm}(\xi_1,\xi_2;z)]^2}$$
$$\times\left[G_0^{\pm}(\xi,\xi_1;z)\left(\frac{1}{\Omega_2}-G_0^{\pm}(\xi_2,\xi_2;z)\right)G_0^{\pm}(\xi_1,\xi';z) + G_0^{\pm}(\xi,\xi_1;z)G_0^{\pm}(\xi_1,\xi_2;z)G_0^{\pm}(\xi_2,\xi';z)\right.$$
$$\left. + G_0^{\pm}(\xi,\xi_2;z)G_0^{\pm}(\xi_2,\xi_1;z)G_0^{\pm}(\xi_1,\xi';z) + G_0^{\pm}(\xi,\xi_2;z)\left(\frac{1}{\Omega_1}-G_0^{\pm}(\xi_1,\xi_1;z)\right)G_0^{\pm}(\xi_2,\xi';z)\right], \quad (9)$$

where we have used the symmetry property, $G_0^{\pm}(\xi_1,\xi_2;z) = G_0^{\pm}(\xi_2,\xi_1;z)$.

IV. COMPLEX POLES

The energy Green's functions $G^{\pm}(\xi,\xi';z)$, as a function of z, have a cut along the entire real axis $(z=E)$. The retarded (advanced) Green's function $G^{+}(\xi,\xi';z)$ $[G^{-}(\xi,\xi';z)]$ is analytic in the upper (lower) half z plane. When we analytically continue $G^{+}(\xi,\xi';z)$ $[G^{-}(\xi,\xi';z)]$ to the lower (upper) half plane, it may have simple poles. The poles can be found from the condition that the denominator of the second term of Eq. (9) becomes zero. If the locations of the poles in the complex z plane are denoted by z_n, then

$$\left(\frac{1}{\Omega_1}-G_0^{\pm}(\xi_1,\xi_1;z_n)\right)\left(\frac{1}{\Omega_2}-G_0^{\pm}(\xi_2,\xi_2;z_n)\right)$$
$$-[G_0^{\pm}(\xi_1,\xi_2;z_n)]^2 = 0. \quad (10)$$

For $G^{+}(\xi,\xi';z)$ $[G^{-}(\xi,\xi';z)]$, the poles are located at $z=z_n$ in the lower (upper) half z plane. Equation (10) must be solved numerically.

The poles of $G^{+}(\xi,\xi';z)$ are plotted in Fig. 2 for values of d and Ω describing O_2^-, and for two different values of the constant external field $F/q=1.43\times10^5$ V/cm and $F/q=7.15\times10^5$ V/cm. In both figures, the single pole located very close to the negative real axis can be associated to the bound state of O_2^-. In the presence of the external constant field, the bound state can tunnel into the continuum and its associated pole energy (the "bound-state" pole) has a small imaginary part, and a real part whose value is close to that of the bound-state energy of the field-free molecule. As we increase the strength of the electric field, this pole moves toward more negative energies, and the difference between the pole's real part and the bound-state energy increases.

The poles along the positive real axis have very small imaginary part and will be called "triangle" poles. They correspond to quasibound states that are created by the triangular potential formed to the left of $\xi=0$ by the electric field potential energy and the delta function located at $\xi=0$. One can check this by calculating the discrete eigenenergies of the triangular well potential composed of a linear field and an infinite wall located at $\xi=0$, and comparing them with real part of the triangle poles. The values are very close. When we increase the strength of the constant electric field, the gap between each triangle pole becomes bigger. This is expected because, as the slope of the electric potential energy is steepened, the discrete energies in the corresponding triangular well potential will move apart. There is also a line of poles that extends into the lower half plane in the third quadrant.

These poles do not have an obvious physical origin although they would not exist if the delta functions were not present.

V. SURVIVAL PROBABILITY

Given Eq. (9) for the retarded energy Green's function $G^+(\xi,\xi';z)$, we can now compute the residue of the pole at $z=z_n$. It is defined $\mathrm{Res}[G^+(\xi,\xi';z)]_{z=z_n}=\lim_{z\to z_n}(z-z_n)G^+(\xi,\xi';z)$. Since $G_0^+(\xi,\xi';z)$ is analytic in the entire complex plane, the contribution to $\mathrm{Res}[G^+(\xi,\xi';z)]_{z=z_n}$ from the first term on the right-hand side vanishes. The contribution from the denominator in the second term in Eq. (9) can be found by L'Hospital's rule and is given by

$$\lim_{z\to z_n}\frac{(z-z_n)}{\left(\frac{1}{\Omega_1}-G_0^+(\xi_1,\xi_1;z)\right)\left(\frac{1}{\Omega_2}-G_0^+(\xi_2,\xi_2;z)\right)-[G_0^+(\xi_1,\xi_2;z)]^2}, \tag{11}$$

$$=\lim_{z\to z_n}\frac{\partial}{\partial z}\frac{1}{\left[\left(\frac{1}{\Omega_1}-G_0^+(\xi_1,\xi_1;z)\right)\left(\frac{1}{\Omega_2}-G_0^+(\xi_2,\xi_2;z)\right)-[G_0^+(\xi_1,\xi_2;z)]^2\right]\Big|_{z=z_n}}. \tag{12}$$

In order to simplify the notation, we define the following quantities $a_n\equiv\frac{1}{\Omega_1}-G_0^+(\xi_1,\xi_1;z_n)$, $b_n\equiv\frac{1}{\Omega_2}-G_0^+(\xi_2,\xi_2;z_n)$, $c_n\equiv G_0^+(\xi_1,\xi_2;z_n)$, and $d_n\equiv\frac{\partial}{\partial z}\{[\frac{1}{\Omega_1}-G_0^+(\xi_1,\xi_1;z)][\frac{1}{\Omega_2}-G_0^+(\xi_2,\xi_2;z)]-[G_0^+(\xi_1,\xi_2;z)]^2\}|_{z=z_n}$ Then the residue can be written as

$$\mathrm{Res}[G^+(\xi,\xi';z)]_{z=z_n}=\frac{1}{d_n}N(\xi,\xi';z_n), \tag{13}$$

where

$$\begin{aligned}N(\xi,\xi';z_n)\equiv&[G_0^+(\xi,\xi_1;z_n)b_nG_0^+(\xi_1,\xi';z_n)\\&+G_0^+(\xi,\xi_1;z_n)c_nG_0^+(\xi_2,\xi';z_n)\\&+G_0^+(\xi,\xi_2;z_n)c_nG_0^+(\xi_1,\xi';z_n)\\&+G_0^+(\xi,\xi_2;z_n)a_nG_0^+(\xi_2,\xi';z_n)].\end{aligned} \tag{14}$$

From the property of the residue $\mathrm{Res}[G^+(\xi,\xi';z)]_{z=z_n}=\psi_{z_n}(\xi)\psi_{z_n}(\xi')$ [11,12] and using Eq. (13), we can write

$$\psi_{z_n}(\xi)\psi_{z_n}(\xi')=\frac{1}{d_n}N(\xi,\xi';z_n). \tag{15}$$

Therefore, using $\psi_{z_n}(0)\psi_{z_n}(0)=\frac{1}{d_n}N(0,0;z_n)$,

$$\psi_{z_n}(\xi)=\frac{1}{\psi_{z_n}(0)}\frac{1}{d_n}N(\xi,0;z_n)=\pm\left(\frac{1}{d_nN(0,0;z_n)}\right)^{1/2}N(\xi,0;z_n). \tag{16}$$

The function $\psi_{z_n}(\xi)$ (whose square is the diagonal element of the residue of the Green's function pole at complex energy z_n) satisfies the equation, $H\psi_{z_n}(\xi)=z_n\psi_{z_n}(\xi)$. For this reason, these functions are called "complex eigenfunctions" in the sense that they have complex eigenvalues. However, they are not square integrable so they do not belong to the Hilbert space of possible physical states (see [12] for more discussion).

Now we can compute the survival probability for the excess electron, in the presence of the constant electric field, when it is initially in the ground state ϕ_0 [see Fig. 1(b)]. The survival probability is defined as $|A(t)|^2$, where $A(t)=\langle\phi_0|\phi(t)\rangle$ is the survival probability amplitude and $|\phi(t)\rangle$ is the state of the excess electron at time t given that it was in the state $|\phi_0\rangle$ at time $t=0$. The survival probability amplitude takes the form (see Appendix)

$$A(t)=\sum_n e^{-iz_nt}\gamma_n\tilde{\gamma}_n^*, \tag{17}$$

where t is understood as the dimensionless time, and γ_n and $\tilde{\gamma}_n^*$ are overlap integrals defined as [12]

$$\gamma_n=\int_{-\infty}^{\infty}d\xi\phi_0^*(\xi)\psi_{z_n}(\xi),$$

$$\tilde{\gamma}_n^*=\int_{-\infty}^{\infty}d\xi\psi_{z_n}(\xi)\phi_0(\xi). \tag{18}$$

Thus, the degree of overlap between the functions $\psi_{z_n}(\xi)$ and the initial condition $\phi_0(\xi)$ determines the extent to which each Green's function pole contributes to the evolution of the survival probability amplitude. For this reason, it is useful to compute the spatial structure of some of the complex eigenfunctions $\psi_{z_n}(\xi)$ numerically from Eq. (16). The real part of the complex eigenfunctions are shown in Fig. 3 for $F/q=1.43\times10^5$ V/cm. We can see that the complex eigenstate corresponding to the "bound-state" pole resembles the bound state $\phi_0(\xi)$ of O_2^-. Using Eq. (17), we can obtain the survival probability numerically.

The survival probability, as a function of time, is plotted in Fig. 4 for external field strength $F/q=1.43\times10^5$ V/cm and $F/q=7.15\times10^5$ V/cm. In both cases, the decay is exponential. This can be explained as follows. In comparing the initial state $|\phi_0\rangle$ in Fig. 1(b) and the complex eigenstate

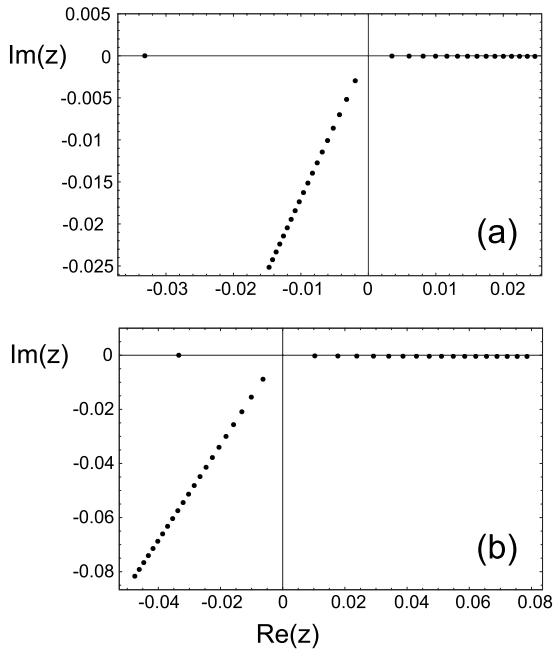

FIG. 2. Poles of the retarded energy Green's function $G^{+}(\xi_1,\xi_2;z)$ for $\Omega=-0.219\,067$, $d=2.281\,88$, and (a) $F/q=1.43\times10^{5}$ V/cm and (b) $F/q=7.15\times10^{5}$ V/cm. The bound-state pole has (dimensionless) complex energy (a) $z=E-i\Gamma=-0.033\,139-5.185\times10^{-16}i$ and (b) $z=E-i\Gamma=-0.033\,416-1.0137\times10^{-14}i$.

in Fig. 3 for $F/q=1.43\times10^{5}$ V/cm, we see that there is a large overlap between the initial state and the complex eigenstate associated with the bound-state pole. It is similar for the $F/q=7.15\times10^{5}$ V/cm case. Thus, the bound-state pole will dominate the time evolution of the survival probability. We can check this by calculating the survival probability coming only from the dominant pole. The survival probability is $P(t)=|A(t)|^2\approx\exp(-2\Gamma t)$, where Γ is the imaginary part of the complex energy for the dominant pole. The width 2Γ is proportional to the inverse lifetime or decay rate for the excess electron. The lifetimes of the electron calculated from the imaginary parts of the complex energies for the dominant poles are about 0.047 and 0.0024 s, which agree well with the decay rates shown in Figs. 4(a) and 4(b), respectively. As we increase the strength of the linear field, the magnitude of the imaginary part becomes bigger, and consequently the lifetime becomes shorter.

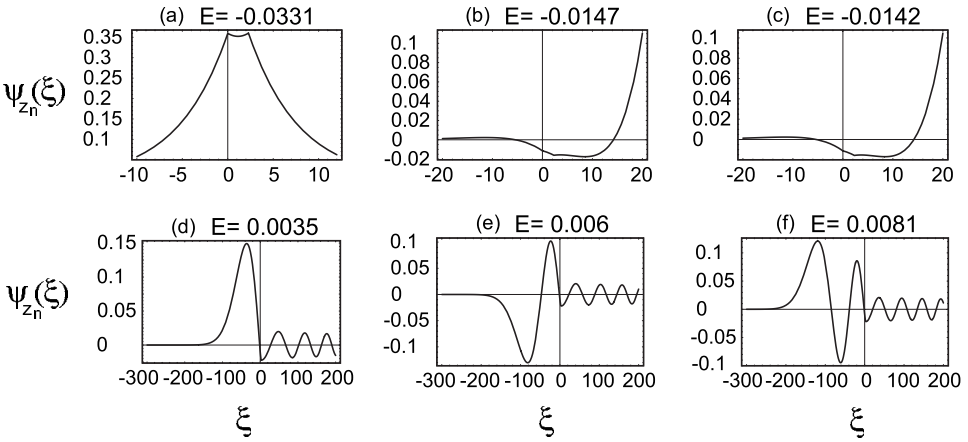

FIG. 3. Real part of complex eigenfunctions for $\Omega=-0.219\,067$, $d=2.281\,88$, and $F/q=1.43\times10^{5}$ V/cm. The number above each plot is the real part of the complex pole corresponding to that function. (a) corresponds to the bound-state pole. (b) and (c) correspond to short-lived poles in the third quadrant. (d)–(f) correspond to triangle poles.

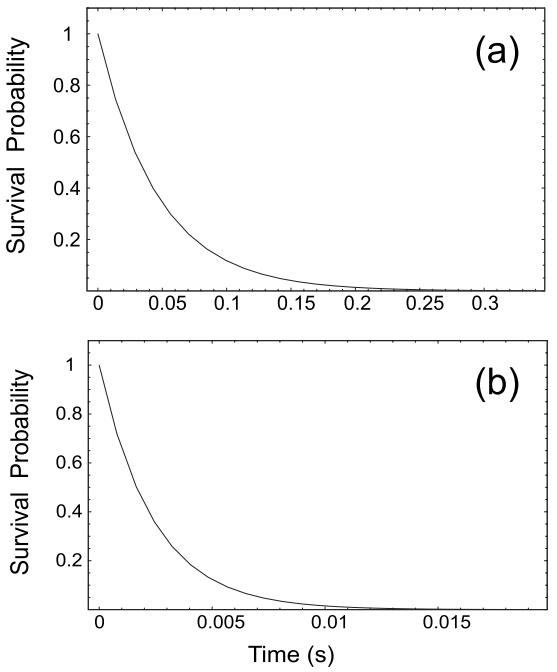

FIG. 4. The survival probability for the initial state shown in Fig. 1(b) with parameters $\Omega=-0.219\,067$, $d=2.281\,88$, and (a) $F/q=1.43\times10^{5}$ V/cm and (b) $F/q=7.15\times10^{5}$ V/cm.

VI. PHOTODETACHMENT RATE

We now compute the photodetachment rate for the excess electron in the presence of the constant electric field with strength F and a radiation field with frequency ω. The Hamiltonian can be written as

$$H(x)=-\frac{\hbar^2}{2m}\frac{d^2}{dx^2}-Fx+V_1\delta(x-x_1)+V_2\delta(x-x_2)+\mathcal{E}qx\cos(\omega t),\tag{19}$$

where $\mathcal{E}$ is the electric field associated with the radiation field, which was chosen so that $\mathcal{E}q$ is one percent of F. If we introduce the dimensionless parameters

$$\mathcal{E}'\equiv\frac{a_0}{\epsilon_0}\mathcal{E}q,\quad \omega'\equiv\frac{\hbar}{\epsilon_0}\omega,\quad\text{and}\quad t'\equiv\frac{\epsilon_0}{\hbar}t,\tag{20}$$

then the total Hamiltonian becomes dimensionless and can be written as

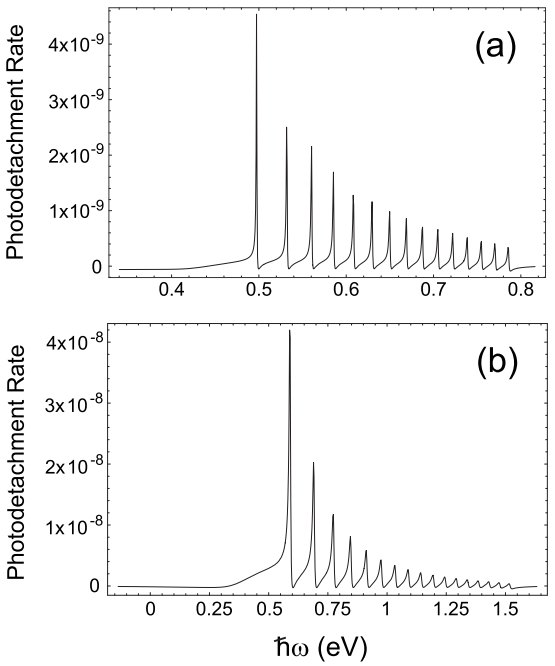

FIG. 5. Photodetachment rate (dimensionless) as a function of radiation field frequency for (a) $F/q=1.43\times10^5$ V/cm and (b) $F/q=7.15\times10^5$ V/cm.

$$H(\xi) = -\frac{d^2}{d\xi^2} - b\xi + \Omega_1\delta(\xi-\xi_1) + \Omega_2\delta(\xi-\xi_2) + \mathcal{E}'\xi\cos(\omega' t'). \tag{21}$$

The dimensionless photodetachment rate W' is (see Appendix)

$$W' = -\frac{\mathcal{E}'^2}{2}\mathrm{Im}\left[\sum_n \frac{\Xi_n}{E_0 \mp \omega' - z_n}\right], \tag{22}$$

where E_0 is understood as dimensionless energy of the initial state, ω' is dimensionless energy of the radiation field, z_n are dimensionless complex poles, and

$$\Xi_n = \left[\int_{-\infty}^{\infty} d\xi\phi_0(\xi)\xi\psi_{z_n}(\xi)\right]^2. \tag{23}$$

We can calculate the photodetachment rate numerically using Eq. (22). Figures 5(a) and 5(b) show the photodetachment rate of the excess electron, as a function of radiation field frequency for constant electric field strengths $F/q=1.43\times10^5$ V/cm and $F/q=7.15\times10^5$ V/cm, respectively. As the strength of the linear field increases, the location of the first peak moves toward higher frequencies, and the gap between each peak becomes wider. We also see a lowering of the threshold of the photodetachment rate, which is 0.45 eV for O_2^-. The threshold lowering is more evident as the strength of the linear field becomes stronger. The peaks in photodetachment occur at the frequencies when the external field energy coincides with the energy difference between quasibound states.

Oscillatory behavior in photodetachment for atomic systems in the presence of a constant external electric field has been ascribed to the interference between the emitted electron wave traveling toward, and reflected from, the potential barrier created by the constant electric field [4]. Due to the lack of experimental data for the molecular ion photodetachment rate with the constant electric field, we could not compare our results with the experiment. However, agreement between the theory and the experiment has been verified for the atomic negative ion (H^-) under the constant electric field [9]. In [4], an approximate calculation that omitted the contribution of the atomic potential to the final state of the electron (but included the effect of the constant field) gave very good agreement between the location and shape of the peaks in the photodetachment rate. The photodetachment peaks in [4] were much broader and lower than those obtained in an exact calculation by [9] using a delta-function potential although the location of the peaks agree. We believe that the reason for the sharper peaks obtained using delta potentials is the following. The delta potential creates a sharp demarcation of the region between the atomic potential and the potential barrier created by the constant field. Thus, quasibound states created by constructive interference of the emitted electron wave in the region of the triangle potential are sharper and longer lived than those created by a broader atomic potential, and this in turn gives rise to sharper peaks in the photodetachment rate. The use of the delta-function potential has the advantage that the calculation of the location of the quasibound states and, therefore, the photodetachment rate peaks is relatively simple.

It is interesting to note that vibrational transition peaks, in addition to electronic transition peaks, have been observed in the photodetachment rate for O_2^- when no linear field is present [10]. We expect that vibrations would add additional peaks to our computed photodetachment rate, in addition to the peaks that are specifically a result of the constant field.

VII. TWO BOUND STATES

If we increase the distance between the two delta functions, two bound states can be formed in the model system (when $b=0$), although the model will no longer describe O_2^-. This gives rise to two bound-state poles (when $b\neq0$) near the negative real axis. As an example, we change the strength of the delta function so that the ground-state energy of the unperturbed system is always the same as the electron affinity of the oxygen molecule. At about four times of the original spacing, the second bound-state pole starts to emerge, and when we further increase the spacing of the two delta functions, the two bound-state poles move closer together. In Fig. 6, we show the pole structure when the spacing between delta functions is $d=13.6913$, which is six times that of O_2^-. If we choose as our initial state, the symmetric bound state of the $b=0$ system when the spacing between delta functions is six times that of O_2^-, the survival probability decays with an exponential envelope but also has small scale oscillations. This is shown in Figs. 7(a) and 7(b). The dominant contribution to the overlap integral in Eq. (18) comes from two quasibound states with complex energies $z_1=E_1-i\Gamma_1=-0.035\ 317-4.3448\times10^{-14}i$ and $z_2=E_2-i\Gamma_2=-0.022\ 601-3.5897\times10^{-8}i$. Then the survival amplitude can be written as

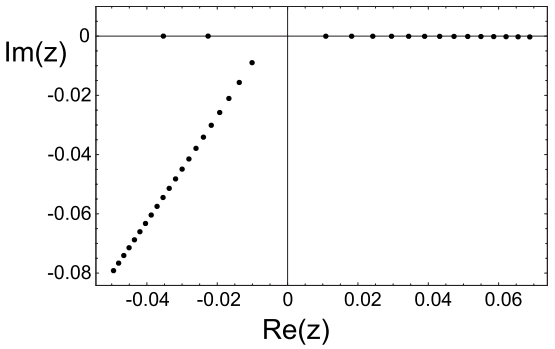

FIG. 6. Complex poles for $F/q=7.15\times10^5$ V/cm, $\Omega=-0.335\,878$, and $d=13.6913$. By increasing the spacing of the two delta functions, two bound-state poles can be formed.

$$A(t)=\sum_n e^{-iz_nt}\gamma_n\tilde{\gamma}_n^*\approx e^{-iz_1t}\gamma_1\tilde{\gamma}_1^*+e^{-iz_2t}\gamma_2\tilde{\gamma}_2^*. \tag{24}$$

Thus, the survival probability is

$$\begin{aligned}P(t)&=|A(t)|^2\\&=|e^{-iE_1t}e^{-\Gamma_1t}\gamma_1\tilde{\gamma}_1^*+e^{-iE_2t}e^{-\Gamma_2t}\gamma_2\tilde{\gamma}_2^*|^2\\&=e^{-2\Gamma_1t}|\gamma_1|^2|\tilde{\gamma}_1^*|^2+e^{-2\Gamma_2t}|\gamma_2|^2|\tilde{\gamma}_2^*|^2\\&\quad+2\,\mathrm{Re}[e^{i(E_2-E_1)t}e^{-(\Gamma_1+\Gamma_2)t}\gamma_1\tilde{\gamma}_1^*\gamma_2^*\tilde{\gamma}_2]\\&=e^{-2\Gamma_1t}|\gamma_1|^2|\tilde{\gamma}_1^*|^2+e^{-2\Gamma_2t}|\gamma_2|^2|\tilde{\gamma}_2^*|^2\\&\quad+2e^{-(\Gamma_1+\Gamma_2)t}R\cos[(E_2-E_1)t+\theta],\end{aligned} \tag{25}$$

where

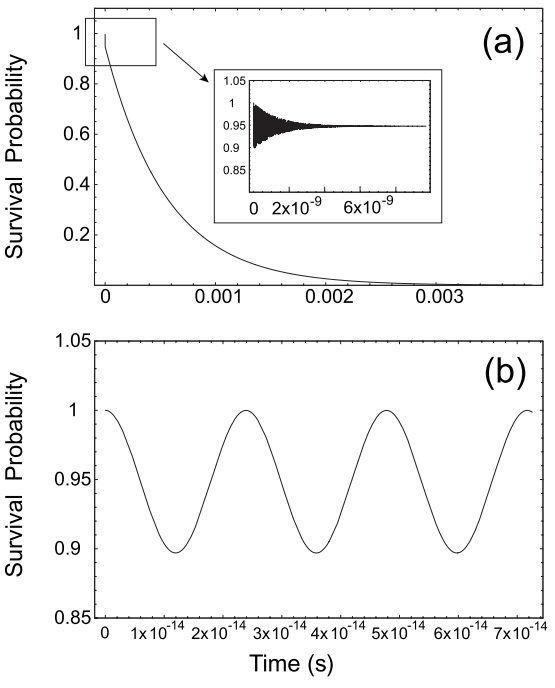

FIG. 7. Survival probability for $\Omega=-0.335\,878$, $d=13.6913$, and $F/q=7.15\times10^5$ V/cm. (a) The exponential envelope (long-time scale). (b) Small scale oscillations (short-time scale).

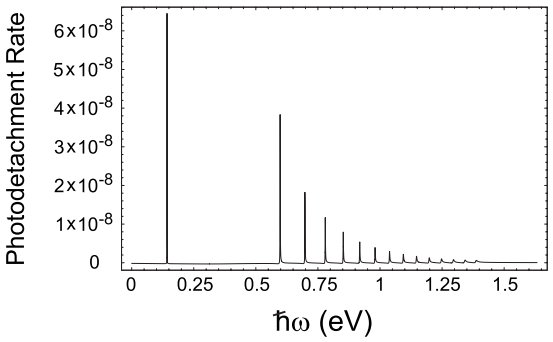

FIG. 8. The photodetachment rate (dimensionless) for $\Omega=-0.335\,878$, $d=13.6913$, and $F/q=7.15\times10^5$ V/cm.

$$R=|\gamma_1\tilde{\gamma}_1^*\gamma_2^*\tilde{\gamma}_2|,\theta=\arg(\gamma_1\tilde{\gamma}_1^*\gamma_2^*\tilde{\gamma}_2). \tag{26}$$

Therefore, the survival probability will show oscillatory decay if several poles contribute to the survival amplitude. The period of the small oscillation in Fig. 7(b) is about 2.39×10^{-14} s and the overall decay lifetime in Fig. 7(a) is about 0.000 557 s. We can also check the lifetime of the small oscillation in the inset of Fig. 7(a), which is determined by $\Gamma_1+\Gamma_2$. In our case Γ_2 is much greater than Γ_1 so Γ_2 dominates the lifetime of oscillation, which is about 1.35×10^{-9} s.

The photodetachment rate shows similar behavior to the case with only one bound-state pole but has peaks at different values and also different spacing between peaks in Fig. 8. It is worthwhile to note the appearance of an additional peak near 0.1425 eV due to the transition between two bound-state poles.

VIII. CONCLUSIONS

The dynamics of the diatomic molecular negative ion, O_2^-, was studied using the complex spectral decomposition of the energy Green's function. Two delta potentials were used to model the atomic potentials at each O atom in this system. The strength of the delta potentials was determined from the O_2^- electron affinity (0.45 eV) and the distance between the delta functions was chosen from the internuclear distance of the diatomic molecule, 1.207 52 Å. Complex poles of the energy Green's function were computed and used to obtain the survival probability and the photodetachment rate. The survival probability of the excess electron in the presence of linear electric field shows exponential decay. The stronger the electric field, the faster the decay. Oscillatory behavior in the decay process is observed when the initial state has large overlap with the residue of two poles of the Green's function. As we change the frequency of the external field, the photodetachment rate shows the peaks where the frequency corresponds to the spacing of the real parts of the complex poles. As the strength of the linear field increases, the location of the first peak moves toward higher frequencies, and the gap between each peak becomes wider. Also, as we increase the linear field strength, we observe the lowering of the threshold of the photodetachment rate. These effects should be observable in an experiment. As explained

earlier, we expect that the use of the delta functions to model the atomic potentials will give rise to sharper photodetachment peaks than those observed in experiment because the actual atomic potential creates a more diffuse triangle potential for quasibound-state formation than does the delta potential. However, ease with which the exact calculations can be done using the delta potentials justifies the use of the delta functions and the accurate predictions for the location of the photodetachment peaks make this approach very useful.

ACKNOWLEDGMENT

The authors wish to thank the Robert A. Welch Foundation (Grant No. F-1051) for support of this work.

APPENDIX

The formula for the survival probability can be derived as follows [12]. The wave function at time $t(t>0)$ can be expressed in terms of the retarded energy Green's function as

$$\phi(x,t) = i\hbar \int_{-\infty}^{\infty} dx' G^R(x,x';t,0)\phi_0(x') = i\hbar \int_{-\infty}^{\infty} dx' \left(\frac{1}{2\pi\hbar} \int_{-\infty+i\epsilon}^{\infty+i\epsilon} dz G(x,x';z) e^{-i(z/\hbar)t} \right) \phi_0(x'). \tag{27}$$

Using contour integral, the integral in the parenthesis can be shown to be a sum of the residues at the poles in the lower half plane. Because the residue at the pole is [11]

$$\mathrm{Res}[G(x,x';z)e^{-i(z/\hbar)t}]|_{z=\varepsilon_n} = \psi_{\varepsilon_n}(x)\psi_{\varepsilon_n}(x')e^{-i(\varepsilon_n/\hbar)t}, \tag{28}$$

the wave function at time t is

$$\phi(x,t) = i\hbar \int_{-\infty}^{\infty} dx' \left(\frac{1}{i\hbar} \sum_n \psi_{\varepsilon_n}(x)\psi_{\varepsilon_n}(x') e^{-i(\varepsilon_n/\hbar)t} \right) \phi_0(x') = \sum_n e^{-i(\varepsilon_n/\hbar)t} \psi_{\varepsilon_n}(x) \int_{-\infty}^{\infty} dx' \psi_{\varepsilon_n}(x')\phi_0(x'), \tag{29}$$

where we used ε_n for the complex poles, which have the dimension of energy in order to distinguish them from the dimensionless complex poles, $z_n = \varepsilon_n/\epsilon_0$. Thus the probability amplitude is

$$\begin{aligned} A(t) &= \langle \phi_0 | \phi(t) \rangle \\ &= \int_{-\infty}^{\infty} dx \langle \phi_0 | x \rangle \langle x | \phi(t) \rangle = \int_{-\infty}^{\infty} dx \phi_0^*(x)\phi(x,t) \\ &= \int_{-\infty}^{\infty} dx \phi_0^*(x) \left(\sum_n e^{-i(\varepsilon_n/\hbar)t} \psi_{\varepsilon_n}(x) \int_{-\infty}^{\infty} dx' \psi_{\varepsilon_n}(x')\phi_0(x') \right) \\ &= \sum_n e^{-i(\varepsilon_n/\hbar)t} \int_{-\infty}^{\infty} dx \phi_0^*(x)\psi_{\varepsilon_n}(x) \int_{-\infty}^{\infty} dx' \psi_{\varepsilon_n}(x')\phi_0(x') \\ &= \sum_n e^{-i(\varepsilon_n/\hbar)t} \gamma_n \tilde{\gamma}_n^* = \sum_n e^{-iz_n t'} \gamma_n \tilde{\gamma}_n^*, \end{aligned} \tag{30}$$

where $t' = (\epsilon_0/\hbar)t$ is dimensionless time, and γ_n and $\tilde{\gamma}_n^*$ are defined as

$$\gamma_n = \int_{-\infty}^{\infty} dx \phi_0^*(x)\psi_{\varepsilon_n}(x) = \int_{-\infty}^{\infty} d\xi \phi_0^*(\xi)\psi_{z_n}(\xi), \tag{31}$$

$$\tilde{\gamma}_n^* = \int_{-\infty}^{\infty} dx \psi_{\varepsilon_n}(x)\phi_0(x) = \int_{-\infty}^{\infty} d\xi \psi_{z_n}(\xi)\phi_0(\xi). \tag{32}$$

The photodetachment rate W can be found as [9]

$$\begin{aligned} W &= \frac{2\pi}{\hbar}\left(\frac{\mathcal{E}q}{2}\right)^2 \int_{-\infty}^{\infty} dE\rho(E)|\langle E|x|\phi_0\rangle|^2 \delta(E - E_0 \pm \hbar\omega) \\ &= \frac{2\pi}{\hbar}\left(\frac{\mathcal{E}q}{2}\right)^2 \int_{-\infty}^{\infty} dx \int_{-\infty}^{\infty} dx' \langle \phi_0|x\rangle x \langle x'|\phi_0\rangle x' \frac{1}{-2\pi i} \sum_n \left[\frac{\langle x|\psi_{\varepsilon_n}\rangle\langle\tilde{\psi}_{\varepsilon_n^*}|x'\rangle}{E_0 \mp \hbar\omega - \varepsilon_n} - \frac{\langle x|\tilde{\psi}_{\varepsilon_n^*}\rangle\langle\psi_{\varepsilon_n}|x'\rangle}{E_0 \mp \hbar\omega - \varepsilon_n^*} \right] \\ &= -\frac{\mathcal{E}^2 q^2}{2\hbar} \mathrm{Im}\left[\int_{-\infty}^{\infty} dx \int_{-\infty}^{\infty} dx' \phi_0(x)x\phi_0(x')x' \sum_n \frac{\psi_{\varepsilon_n}(x)\psi_{\varepsilon_n}(x')}{E_0 \mp \hbar\omega - \varepsilon_n} \right] = -\frac{\epsilon_0}{\hbar}\frac{\mathcal{E}'^2}{2} \mathrm{Im}\left[\sum_n \frac{\Xi_n}{(E_0/\epsilon_0) \mp (\hbar\omega/\epsilon_0) - z_n} \right], \end{aligned} \tag{33}$$

where ε_n and z_n are defined as above, and

$$\Xi_n = \left(\frac{1}{a_0} \int_{-\infty}^{\infty} dx \phi_0(x)x\psi_{\varepsilon_n}(x) \right)^2 = \left[\int_{-\infty}^{\infty} d\xi \phi_0(\xi)\xi\psi_{z_n}(\xi) \right]^2. \tag{34}$$

Thus, dimensionless photodetachment rate W' is

$$W' = \left(\frac{\epsilon_0}{\hbar}\right)^{-1} W = -\frac{\mathcal{E}'^2}{2} \mathrm{Im}\left[\sum_n \frac{\Xi_n}{(E_0/\epsilon_0) \mp (\hbar\omega/\epsilon_0) - z_n} \right]. \tag{35}$$

[1] H. C. Bryant, A. Mohagheghi, J. E. Stewart, J. B. Donahue, C. R. Quick, R. A. Reeder, V. Yuan, C. R. Hummer, W. W. Smith, S. Cohen, W. P. Reinhardt, and L. Overman, Phys. Rev. Lett. **58**, 2412 (1987).
[2] J. E. Stewart, H. C. Bryant, P. G. Harris, A. H. Mohagheghi, J. B. Donahue, C. R. Quick, R. A. Reeder, V. Yuan, C. R. Hummer, W. W. Smith, and S. Cohen, Phys. Rev. A **38**, 5628 (1988).
[3] P. G. Harris, H. C. Bryant, A. H. Mohagheghi, C. Tang, J. B. Donahue, C. R. Quick, R. A. Reeder, S. Cohen, W. W. Smith, J. E. Stewart, and C. Johnstone, Phys. Rev. A **41**, 5968 (1990).
[4] N. D. Gibson, B. J. Davies, and D. J. Larson, Phys. Rev. A **48**, 310 (1993).
[5] I. I. Fabrikant, Zh. Eksp. Teor. Fiz. **79**, 2070 (1980).
[6] A. R. P. Rau and H. Y. Wong, Phys. Rev. A **37**, 632 (1988).
[7] H. Y. Wong, A. R. P. Rau, and C. H. Greene, Phys. Rev. A **37**, 2393 (1988).
[8] M. L. Du and J. B. Delos, Phys. Rev. A **38**, 5609 (1988).
[9] A. Emmanouilidou and L. E. Reichl, Phys. Rev. A **62**, 022709 (2000).
[10] R. J. Celotta, R. A. Bennett, J. L. Hall, M. W. Siegel, and J. Levine, Phys. Rev. A **6**, 631 (1972).
[11] A. Ludviksson, J. Phys. A **20**, 4733 (1987).
[12] J. C. Nickel and L. E. Reichl, Phys. Rev. A **58**, 4210 (1998).
[13] S. Gasiorowicz, *Quantum Physics* (John Wiley and Sons, Inc., New York, 1974), p. 94.
[14] D. R. Lide, *CRC Handbook of Chemistry and Physics*, 88th ed. (CRC Press, Boca Raton /Taylor and Francis, London, 2008).